

## Article

# A Novel H<sub>2</sub>O/LiBr Absorption Heat Pump with Condensation Heat Recovery for Combined Heating and Cooling Production: Energy Analysis for Different Applications

Juan Prieto \* , Dereje S. Ayoub and Alberto Coronas 

Mechanical Engineering Department CREVER, Universitat Rovira i Virgili, Avda. Països Catalans 26, 43007 Tarragona, Spain

\* Correspondence: juan.prieto@urv.cat; Tel.: +34-680-151-827

**Abstract:** The aim of this study is to analyze the feasibility of the single-effect H<sub>2</sub>O/LiBr absorption heat pump cycle to produce combined heating and cooling. To achieve this, first, the main changes that the absorption cycle requires are described in comparison with the conventional single-effect absorption chiller. Then, the cycle's operational limits in terms of temperature lift and LiBr crystallization are evaluated. In this sense, driving heat temperatures required for these applications range from 85 °C to 120 °C. The energy and exergy performance (in terms of cooling and heating capacities, cooling and heating coefficient of performance, and exergy coefficient of performance) of the cycle is theoretically studied for five different types of applications that require simultaneous heating and cooling: building air conditioning, a 4th generation district heating and cooling network, a sports center with an indoor swimming pool, a hybrid air conditioning system with an absorption heat pump and a desiccant evaporative cooling system, and simultaneous cooling and water purification application for coastal areas. The system performance in terms of the cooling coefficient of performance varies in the range of 0.812–0.842, in terms of heating coefficient of performance from 0.58 to 1.842, and in terms of exergy coefficient of performance from 0.451 to 0.667. The application with the highest exergy coefficient of performance is the 4th generation district heating and cooling network.

**Keywords:** energy analysis; absorption heat pump; H<sub>2</sub>O/LiBr; combined heating and cooling



**Citation:** Prieto, J.; Ayoub, D.S.; Coronas, A. A Novel H<sub>2</sub>O/LiBr Absorption Heat Pump with Condensation Heat Recovery for Combined Heating and Cooling Production: Energy Analysis for Different Applications. *Clean Technol.* **2023**, *5*, 51–73. <https://doi.org/10.3390/cleantechnol5010004>

Academic Editor: Patricia Luis

Received: 14 October 2022

Revised: 15 November 2022

Accepted: 23 December 2022

Published: 31 December 2022



**Copyright:** © 2022 by the authors. Licensee MDPI, Basel, Switzerland. This article is an open access article distributed under the terms and conditions of the Creative Commons Attribution (CC BY) license (<https://creativecommons.org/licenses/by/4.0/>).

## 1. Introduction

In Europe, heating and cooling account for almost 50% of the total final energy consumption [1]. Most of the heating and cooling demands are in buildings and industries. Despite rising cooling demand in Europe, most of the energy consumed is still for heating purposes with fossil fuels used as the dominant primary energy source. The building stock is responsible for 40% of total energy consumption and 36% of all greenhouse gas (GHG) emissions in the European Union (EU) [2]. Therefore, the decarbonization of the heating and cooling sector is crucial to reaching the EU's climate neutrality goal by 2050 and the prior target set to reduce net GHG emissions by at least 55% by 2030 [1]. The replacement of fossil fuels with renewable energy sources and deployment of low-carbon technologies, such as heat pumps (HPs), in the heating and cooling sector has been slower to date, especially in contrast to renewable electricity generation. Furthermore, the transition to sustainable heating and cooling is an appealing challenge considering the current geopolitics in the EU energy landscape. Thus, heat pumping technology is key to linking the use of renewable energy sources and energy efficiency in the heating and cooling sectors. Thereby, the implementation of HPs enables a faster transition of buildings and industrial users from dependence on fossil fuels for heating and cooling applications.

Heat pumping technologies are often limited to either the provision of heating or cooling (as a refrigerator or chiller) even though HPs can be designed to supply heating and cooling simultaneously with the right choice of working fluid (refrigerant) and the

design of system components. Moreover, a considerable amount of heating and cooling are required simultaneously or within a short span in the building sector, food processing industries, and other applications. For instance, simultaneous heat and cold productions are required in hotels for space cooling and domestic hot water (DHW) production [3,4]; in office buildings for server room cooling and space heating; swimming pool heating and ice rink cooling in sports complexes [5]; in the food processing industries (e.g., the dairy processing industry) for product refrigeration, process heating and cooling, and hot water for cleaning purposes [6–8]; and other applications, such as space cooling and seawater desalination, for example, in coastal areas [9]. Therefore, HPs capable of delivering heat and cold simultaneously have advantages in these types of buildings and industrial applications compared to separate production of heat and cold from the viewpoint of efficient utilization of primary energy sources. Besides, conventional heating and cooling systems (e.g., natural gas boiler and electricity-driven vapor compression chiller, respectively) used in these types of applications consume more primary energy than the combined production of heating and cooling using a single heat pump.

The heat pumping technologies are classified as work-driven and heat-driven HPs based on the type of driving input energy, which is electrical/mechanical energy and thermal energy, respectively. Among the heat-driven HPs, this study is focused on absorption heat pumps (AHPs) for simultaneous heating and cooling supply for potential applications in the building and industrial sectors. In the literature, various researchers have carried out theoretical and experimental studies on AHP cycles that combine cooling and heating (or water purification using the heating output to drive thermal separation processes) applications, and consequently, before presenting the proposed AHP concept in this paper, selected related studies are highlighted below.

The earliest AHP cycle configuration proposed for the combined heating and cooling production dates back to the 1980s, using an H<sub>2</sub>O/LiBr working pair by Eisa et al. [10]. The thermodynamic design data for the potential combinations of operating temperatures of the absorber (30–50 °C), condenser (50–100 °C), evaporator (2–15 °C), and generator (70–170 °C) of the single-effect H<sub>2</sub>O/LiBr AHP cycle were obtained using simulation and reported taking into consideration of the LiBr crystallization limit in the absorber and generator. Further, Kumar et al. [11] carried out an experimental study on the single-effect H<sub>2</sub>O/LiBr AHP for combined heating and cooling production taking advantage of the heat released during the absorption and condensation processes. Best et al. [12] also conducted a similar study using an NH<sub>3</sub>/LiNO<sub>3</sub> working pair and obtained the AHP cycle thermodynamic design data for the feasible combination of operating temperatures of the absorber (50–100 °C), condenser (50–100 °C), evaporator (−10–+15 °C), and generator (90–170 °C) with NH<sub>3</sub> concentration in the range of 30 to 55%. The same type of study was continued for the single-effect AHP cycle with H<sub>2</sub>O/Carrol (LiBr + ethylene glycol, ratio 4.5) working pair by Best et al. [13] and the corresponding thermodynamic design data were obtained for the feasible operating temperature range of the absorber (30–50 °C), condenser (50–100 °C), evaporator (2–14 °C), and generator (80–160 °C). These studies examined the potential of the single-stage AHP cycle using several types of working fluid mixtures (H<sub>2</sub>O/LiBr, H<sub>2</sub>O/Carrol, and NH<sub>3</sub>/LiNO<sub>3</sub>) for the combined production of heating and cooling for a range of operating conditions. In these AHP cycles, the condenser heat is released at temperature levels suitable for various applications, while the cooling is delivered by the evaporator for a range of temperatures.

The use of heat rejected by the condenser of the AHPs for desalination and water purification applications using thermal separation processes in closed- and open-loop integrated AHPs was studied by some researchers. Solar-driven H<sub>2</sub>O/LiBr AHP coupled with a multi-effect distillation (MED) system with up to eight effects was proposed and modeled for both cooling production and water purification [14]. The vapor leaving the desorber (generator) of the H<sub>2</sub>O/LiBr AHP was used to drive the MED system and the condensate from the first three effects of the MED system was utilized in the evaporator of the AHP to provide the cooling output. The cooling COP of the AHP cycle reaches

about 0.743, and the overall COP of the combined AHP–MED system could reach 1.44. The heat rejected from the absorber and condenser of a solar-driven H<sub>2</sub>O/LiBr AHP was used to deliver the required warm water for the humidification–dehumidification (HDH) process to provide water purification while delivering a cooling effect at the evaporator [15]. Using this coupled system, a daily water production of 5–9 L was obtained per unit area of solar collector array during the summer season, which is about twice the water production capacity of typical solar still. Another desalination system, based on a vacuum-enhanced distillation process, using the heat rejected from the H<sub>2</sub>O/LiBr AHP as a driving heat source was theoretically investigated [16]. This hybrid solar-assisted cooling and desalination system was able to provide 3.25 kW of cooling with a desalinated water production capacity of 4.5 kg/h.

The vapor generated by the desorber of H<sub>2</sub>O/LiBr AHP was utilized to drive a MED system with six effects in the cycle configuration developed by Wang and Lior [17–19]. In this combined AHP–MED system, the MED system's first effect was utilized as a condenser of the AHP with the condensate provided to the AHP's evaporator for obtaining the cooling output. Furthermore, they studied a cycle modification in which a second absorber was utilized for absorbing the vapor generated in the last effect of the MED system, and the heat rejected by this absorption process was used as extra steam to drive the MED system [17,18]. The modified system was capable of providing flexibility in the ratio of cooling to freshwater production. Ibrahim and Dincer [20] designed and developed a combined system comprising an intermittent H<sub>2</sub>O/LiBr AHP and a solar still to provide both cooling and desalinated water for domestic applications in rural areas. The combination between the seawater desalination system and the AHP system (i.e., for cooling production) is by using seawater as a coupling fluid for the condenser, evaporator, and absorber. The produced cooling effect, as chilled water, was stored in a storage tank to supply the cooling for a conditioned space during the day due to the intermittent operation of the AHP. This solar-driven combined system operated with an energy efficiency of around 13.8% and maximum desalination unit efficiency of about 40%.

Boman and Garimella [21,22] recently investigated an open-loop H<sub>2</sub>O/LiBr AHP cycle combined with membrane-based water purification processes (i.e., membrane distillation (MD) and forward osmosis (FO)) to provide simultaneous graywater purification and space cooling/heating. The thermodynamic model of combined open-loop cycles (i.e., H<sub>2</sub>O/LiBr AHP-MD or H<sub>2</sub>O/LiBr AHP-FO) was developed and applied to analyze the performance of the cycle over a wider range of water loads [21]. Moreover, the performance of the combined cycle in cooling and heating modes of operation were studied at varied evaporator temperatures (3–25 °C), water loads (up to 1000 kg/day), and graywater inlet temperatures (5–23 °C) of the cycle based on MD process [21]. The performance of the MD-based cycle was higher than the FO-based cycle at a high-water demand regime in both heating and cooling modes of operation. Moreover, they designed, modeled, and experimentally validated a horizontal-tube (length of 0.24 m) falling-film heat exchanger to serve as absorber (or desorber) of the open-loop H<sub>2</sub>O/LiBr AHP with a small-scale cooling output (0.3 kW) and a water purification capacity of ~10.5 kg/day [22]. Two feed solutions (i.e., synthetic graywater and 3.5 wt% NaCl solution) representative of unconventional water sources were tested in their experimental study to evaluate the performance of the proposed water purifying H<sub>2</sub>O/LiBr AHP concept, and it allows for the removal of 90% of contaminants from the synthetic graywater and 99% of NaCl from the feed NaCl solution.

Based on the above-reviewed studies, the following research gaps were identified:

- The performance of a single-stage H<sub>2</sub>O/LiBr AHP for simultaneous heating and cooling supplies for different types of potential end-use applications was not investigated;
- The feasibility of utilizing heat rejected during the condensation process of a single-effect H<sub>2</sub>O/LiBr chiller for heating applications at different temperature levels was not analyzed except in some previous cycle thermodynamic studies;
- The majority of previously studied H<sub>2</sub>O/LiBr AHP cycles for combined heating and cooling have been focused on energy analysis in terms of COPs, and this type of system requires the consideration of both

quantity and quality of the dual useful outputs (i.e., heating and cooling capacities and heating and cooling supply temperatures) in their performance evaluation.

In this paper, the feasibility of a new single-effect H<sub>2</sub>O/LiBr AHP cycle configuration for the combined production of cooling and heating at several temperature levels is investigated. Thereby, the new H<sub>2</sub>O/LiBr AHP cycle can be integrated with several types of end-use applications. First, the main difference of this AHP cycle configuration is described in contrast to the conventional single-effect H<sub>2</sub>O/LiBr chiller. Then, the numerical model of the AHP cycle is developed and the operational limits of the cycle in terms of temperatures are identified; thus, it is used to set the suitable potential applications of the proposed cycle configuration. Finally, the performance of the AHP for various applications is evaluated based on its cooling capacity, heating capacity, coefficient of performance (COP), and exergy COP (ECOP).

## 2. System Description

### 2.1. Cycle Description

The proposed absorption heat pump (AHP) configuration (which is already filed as a patent application together with Senso Renoval S.L., Madrid, Spain) is based on a single-effect absorption H<sub>2</sub>O/LiBr chiller with its cycle modification to recover the heat of condensation at a useful temperature level. Thereby, the performance of the AHP is improved (i.e., higher energy utilization efficiency) and enables the delivery of multiple useful outputs simultaneously (e.g., space cooling, heating, and domestic hot water (DHW)). Furthermore, the heat of condensation is also used internally for the LiBr solution preheating to reduce the generator heat input. Figure 1 shows a schematic layout of the proposed single-effect H<sub>2</sub>O/LiBr AHP for combined cooling and heating applications. As can be seen in Figure 1, two new components are incorporated for the co-production of heating/preheating in the conventional single-effect H<sub>2</sub>O/LiBr chiller: a preheater (PH) and a water–solution heat exchanger (WSHX). The weak, in LiBr, solution is preheated (stream 2 to 19) before entering the solution heat exchanger (SHX) by using the heat released during condensation of part of the vapor leaving the generator (stream 7). The PH is implemented in parallel with the condenser (C). The WSHX cools the strong, in LiBr, solution leaving the SHE (stream 5 to 20) while producing hot water (stream 21 to 22) for various end-use applications (e.g., DHW). Moreover, the heat released by the condenser (stream 15 to 16) is at a useful temperature level so that it can be used for heating applications.

Apart from the added new components (i.e., PH and WSHX), the operational conditions of the proposed H<sub>2</sub>O/LiBr AHP (Figure 1) are considerably altered in contrast to the conventional single-effect H<sub>2</sub>O/LiBr chiller. Figure 2 illustrates the Dühring plot of the single-effect H<sub>2</sub>O/LiBr AHP with the recovery of condensation heat, in which its cyclic process is denoted by red lines (stream 1 to 10, stream 19 and 20).

The AHP cycle operates at two pressure levels (i.e., low and high pressures). The AHP cycle low pressure, about 1 kPa, is corresponding to the evaporator and absorber pressures, which is similar to the conventional single-effect absorption chiller with an evaporator temperature of 7.5 °C. On the other hand, the cycle's high pressure (related to the condenser, generator, preheater, SHX, and WSHX operating pressures) is about twofold, about 16.5 kPa, of the conventional H<sub>2</sub>O/LiBr cooling cycle when the condenser rejects heat at 40 °C. The condensation temperature depends on the high pressure; hence, condensation heat recovery at higher temperatures can be realized by increasing the cycle's high pressure. Thus, it allows the utilization of the heat of condensation for heating applications and preheating of the weak LiBr solution.

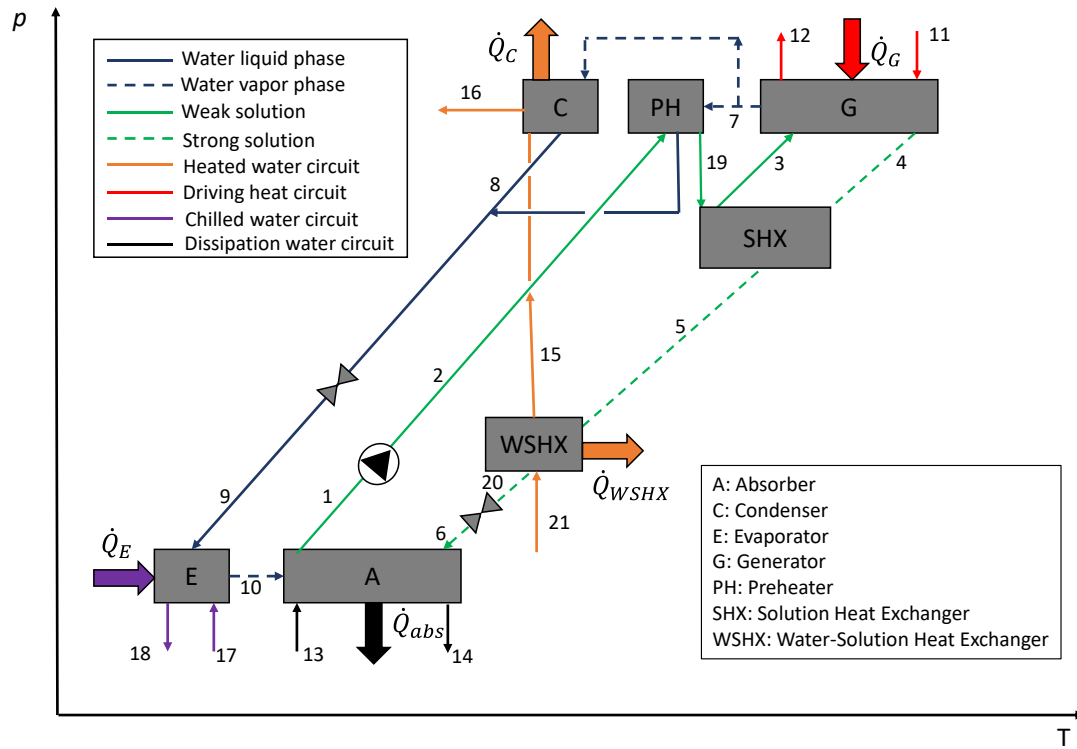


Figure 1. Proposed single-effect H<sub>2</sub>O/LiBr absorption heat pump for combined heating and cooling production.

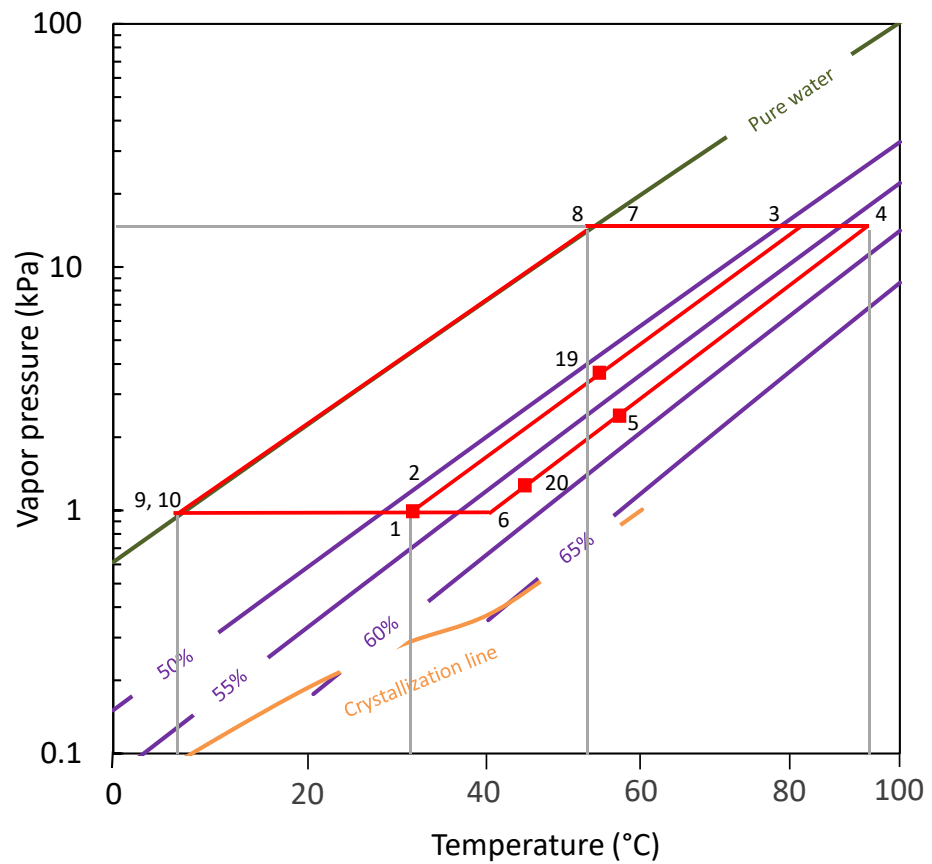


Figure 2. Dühring plot for the proposed single-effect H<sub>2</sub>O/LiBr absorption heat pump with condensation heat recovery.

Table 1 contains the AHP operating conditions referring to Figure 2, for the streams 1 to 10 and 19 to 20.

**Table 1.** AHP operating conditions referring to Figure 2.

State Points	$\dot{m}_i$ (kg · s <sup>-1</sup> )	$T_i$ (°C)	$p_i$ (kPa)	$h_i$ (kJ · kg <sup>-1</sup> )	$q_i$ (-)	$x_i$ (-)	$s_i$ (kJ · kg <sup>-1</sup> · K <sup>-1</sup> )
1	1.000	33.0	1.04	73.0	0.000	0.5304	0.212
2	1.000	33.0	16.53	73.0	0.000	0.5304	0.212
3	1.000	89.3	16.53	192.6	0.000	0.5304	0.570
4	0.929	96.0	16.53	214.4	0.000	0.5707	0.566
5	0.929	57.1	16.53	135.9	0.000	0.5707	0.340
6	0.929	40.4	1.04	102.3	0.000	0.5707	0.237
7	0.0706	87.7	16.53	2663.0	1.000	0.0000	8.151
8	0.0706	56.0	16.53	234.4	0.000	0.0000	0.781
9	0.0706	7.5	1.04	234.4	0.082	0.0000	0.837
10	0.0706	7.5	1.04	2515.0	1.000	0.0000	8.962
19	1.000	55.0	16.53	119.6	0.000	0.5304	0.357
20	0.929	40.4	16.53	102.3	0.000	0.5707	0.236

Besides the change in the high pressure, the proposed AHP cycle (Figure 1) operates at four temperature levels instead of three temperature levels, which is the typical operating condition in the case of a conventional single-effect H<sub>2</sub>O/LiBr absorption chiller:

- In the evaporator, where the cooling effect is produced, the temperature is in the range of 5 °C to 15 °C as in conventional single-effect H<sub>2</sub>O/LiBr absorption chillers.
- In the absorber, heat is released at a temperature in the range of 25 °C to 40 °C, which is comparable to the conventional single-effect absorption chillers. At these temperature levels, the heat is rejected to the environment (e.g., ambient air) since it cannot be used for most heating applications.
- In the condenser, the heat is released between 50 °C and 68 °C. Therefore, the rejected heat can be used for various types of heating applications.
- In the generator, the driving heat of the AHP is in the range of 85 °C to 120 °C.

As can be seen in Figure 2, the cycle is far from the LiBr crystallization line (stream 6) and, therefore, the risk of crystallization at these operating conditions is minimized. Hence, the operational conditions are not as constricted as in the conventional cycle. Especially, the generator temperatures can be much higher in this case.

Additionally, as the solution is preheated (stream 2 to 19) before entering the SHX, the temperature of the strong solution leaving the SHX (stream 5) is higher in this AHP cycle, which allows for the production of extra useful heat by including a liquid–liquid heat exchanger (WSHX, Figure 1) in the cycle. The LiBr mass fraction difference between the weak and the strong solutions is smaller in this cycle than in the conventional H<sub>2</sub>O/LiBr chiller, so it is necessary to increase the solution flow rate to achieve the same amount of cooling and heating, which needs a larger solution pump.

Moreover, since the risk of crystallization is avoided, the SHX effectiveness ( $\eta_{HX}$ ) can be increased so that it improves the cycle COP. The effect of the SHX effectiveness on the cooling COP ( $COP_C$ ), the heating COP ( $COP_H$ ), and the exergy COP ( $ECOP$ ) is shown in Figure 3. As it can be observed, the higher the  $\eta_{HX}$ , the higher the  $COP_C$ . The total  $COP_C$  increase is 17.7% when the  $\eta_{HX}$  is increased from 0.50 to 0.95. This increase is mainly due to a lower heating required in the generator. On the other hand, the higher the  $\eta_{HX}$ , the slightly lower the  $COP_H$ . The total  $COP_H$  decrease is 3.1% when the  $\eta_{HX}$  is increased from 0.50 to 0.95. This decrease is mainly due to a lower heating available in the WSHX. The combination of both effects leads to an increase of the  $ECOP$  from 4.1% for the same range of  $\eta_{HX}$ .

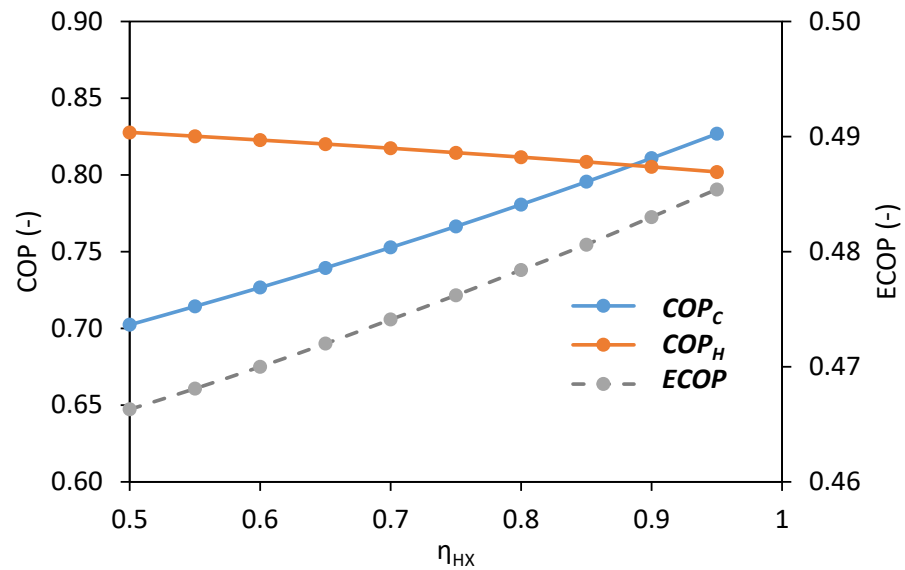


**Figure 3.** AHP  $COP_C$ ,  $COP_H$ , and  $ECOP$  as function of the SHX effectiveness.

In summary, these are the main differences between the conventional and the proposed absorption cycles, and their influence on the cycle's performance and operating conditions:

- The high pressure of the absorption cycle is raised to increase the condensation temperature to a useful level.
- The strong LiBr solution mass fraction is decreased, which minimizes the risk of LiBr crystallization.
- The solution flow rate is increased to achieve the same cooling production.
- The SHX effectiveness is increased so that the absorption cycle performance is improved.
- A preheater is included for weak solution preheating by using part of the recovered heat of condensation.
- A WSHX is included to cool the strong LiBr solution temperature and increase the heating production of the system.
- All these changes lead to the provision of combined heating and cooling and increase the overall performance of the system.

In addition to the heating provided by the water–solution heat exchanger and the condenser, heating could also be obtained from the absorber, if the end-use application would require heating at low temperatures below 40 °C. This fact would even further increase the AHP cycle efficiency.

To better illustrate the changes of the proposed single-effect AHP cycle in comparison to the conventional single-effect H<sub>2</sub>O/LiBr cooling cycle, Figure 4 shows the Dühring plot of both cycles. The conventional cycle is represented by black lines, while the red lines denote the proposed single-effect AHP cycle for combined heating and cooling outputs. As can be seen in Figure 4, for the same temperature levels in the absorber, evaporator, and generator the proposed cycle operates with higher system high pressure, lower strong solution LiBr mass fraction, and further away from the crystallization region.

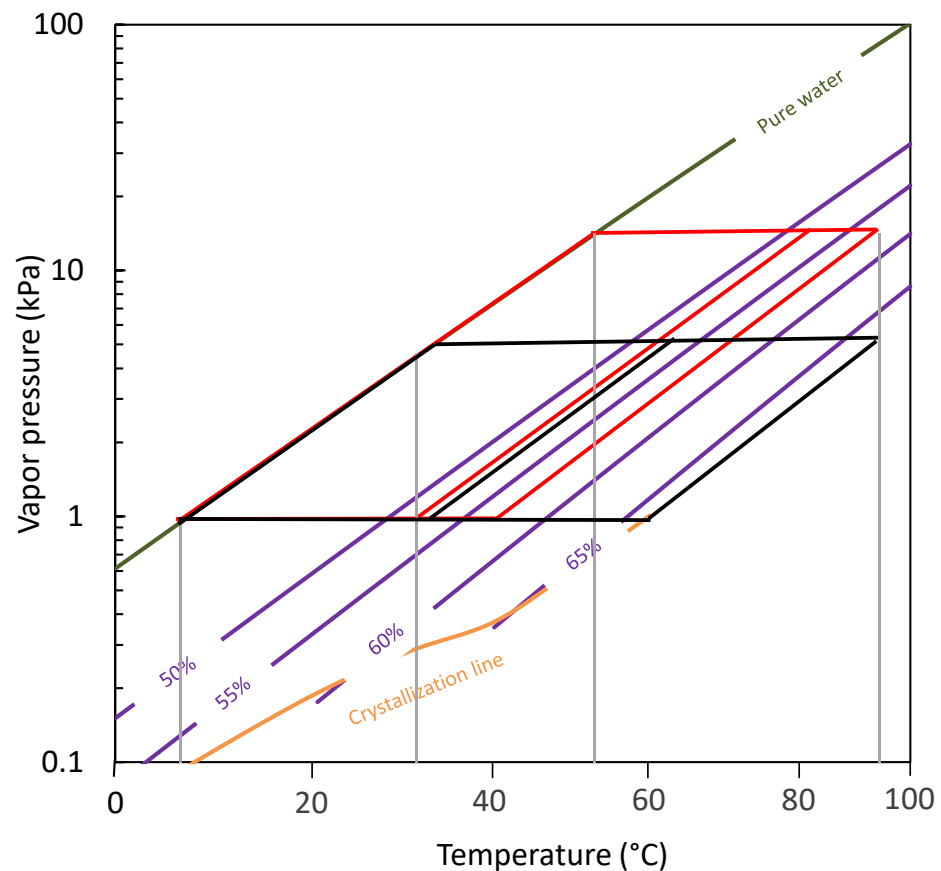


**Figure 4.** Dühring plot for the conventional single-effect H<sub>2</sub>O/LiBr absorption chiller and the proposed single-effect H<sub>2</sub>O/LiBr heat pump for combined heating and cooling.

## 2.2. Operational Limits of the Cycle

The H<sub>2</sub>O/LiBr AHP cycle operational conditions are limited by: (i) the minimum driving heat temperature to activate the cycle; and (ii) the risk of LiBr crystallization during varied operating conditions. Thereby, since the proposed single-effect H<sub>2</sub>O/LiBr AHP cycle is changed compared to the conventional single-effect H<sub>2</sub>O/LiBr absorption chiller, it is desirable to analyze the new operational range of the proposed AHP cycle. Figure 5 shows the minimum and maximum driving heat temperatures as a function of the heat supply temperature and the absorber cooling water inlet temperature for a chilled water supply temperature of 10 °C (left graph) and 15 °C (right graph). As can be seen from this Figure, the maximum driving heat temperature is mainly affected by the heat supply temperature. The higher the heat supply temperature, the higher the maximum driving heat temperature. This effect is due to the higher pressures of the cycle and the subsequent lower strong solution LiBr mass fractions. The minimum driving heat temperature is dependent on the absorber inlet cooling water temperature and the hot water and chilled water supply temperatures. The lower the chilled water supply temperature, the higher the absorber cooling water inlet temperature, and the higher the hot water supply temperature, the higher the required minimum driving heat temperature. This is mainly due to two effects:

The first effect is similar to the conventional single-effect absorption cycle, the chilled water supply temperature and the absorber cooling water inlet temperature determine the weak solution mass fraction and, consequently, the minimum driving heat temperature of the absorption cycle.

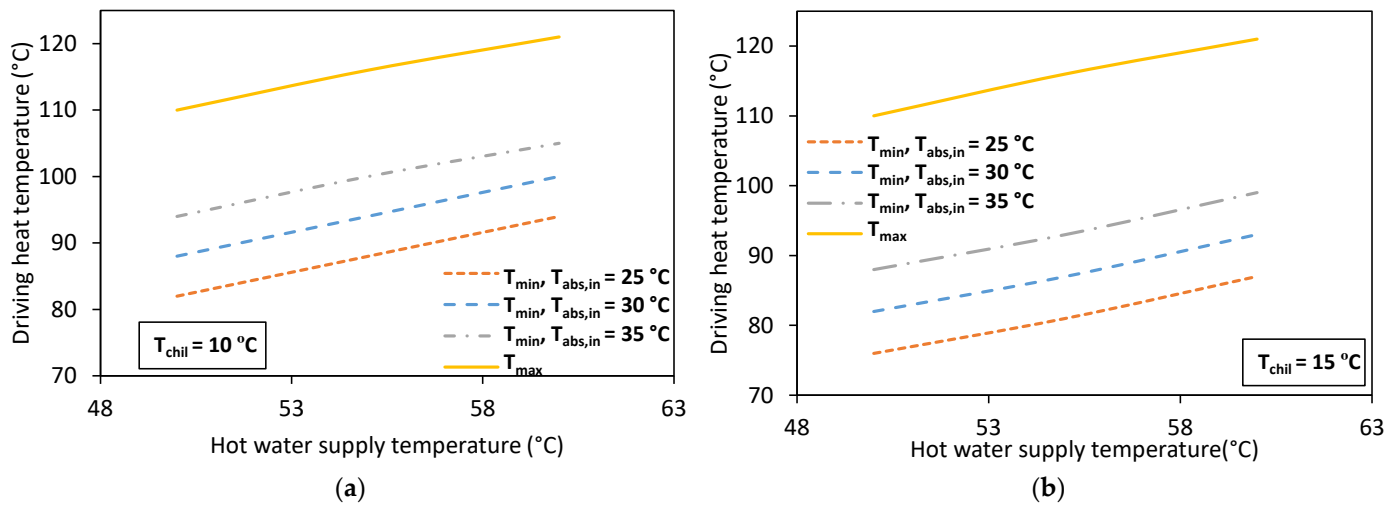


**Figure 5.** Minimum and maximum driving heat temperatures as function of the hot water supply temperature and absorber cooling water inlet temperature for a chilled water supply temperature of 10 °C (a) and 15 °C (b).

The second effect is due to the higher pressure in the condenser and generator, which implies a higher driving heat temperature to generate vapor. The maximum temperature ( $T_{max}$ ) and the minimum temperatures ( $T_{min}$ ) increase following a similar trend as function of the hot water supply temperature. Therefore, the higher the chilled water supply temperature, the wider the AHP operating range, independently of the hot water supply temperature.

Therefore, the driving heat temperatures required for the proposed range from 85 °C to 120 °C. These temperatures are higher than for the single-effect absorption cycle, whose driving heat temperatures range from 80 °C to 100 °C.

### 3. Potential Applications

In order to evaluate the technical feasibility of the presented H<sub>2</sub>O/LiBr AHP for simultaneous heating and cooling, it is evaluated for five different potential applications:

- Simultaneous heating and cooling for building air conditioning.
- Simultaneous heating and cooling for 4th Generation District Heating and Cooling Networks (DHC).
- Simultaneous heating and cooling for a sports center with an indoor swimming pool.
- Hybrid air conditioning system with an absorption heat pump and a desiccant evaporative cooling system.
- Simultaneous cooling and water purification for small-scale remote region applications.

In the following subsections the applications and the AHP integration are described in detail.

#### 3.1. Simultaneous Heating and Cooling for Air Conditioning

The first application is the provision of simultaneous heating and cooling for air conditioning in buildings. Figure 6 illustrates how the proposed heat pump is integrated for this application. The AHP is providing chilled water at 10 °C and hot water at 50 °C to the air conditioning system. These temperatures are suitable for a four-tube fan coil air conditioning system. The return temperatures of the system are 15 °C and 40 °C for the chilled and hot water circuits, respectively. The heat released during the absorption process, in the absorber, of this design cannot be used as useful heat for this application as temperature requirements for heating (i.e., 50 °C) are higher than that provided by it, which is 35 °C. Therefore, the heat released by the absorber should be dissipated through a cooling tower. In this case, hot water passes first through the water–solution heat exchanger

and then through the condenser. The hot water temperature required for the driving heat is 95 °C. Therefore, the heating source for the absorption chiller activation can be provided by low-temperature solar thermal collectors, boilers, geothermal energy, or waste heat.

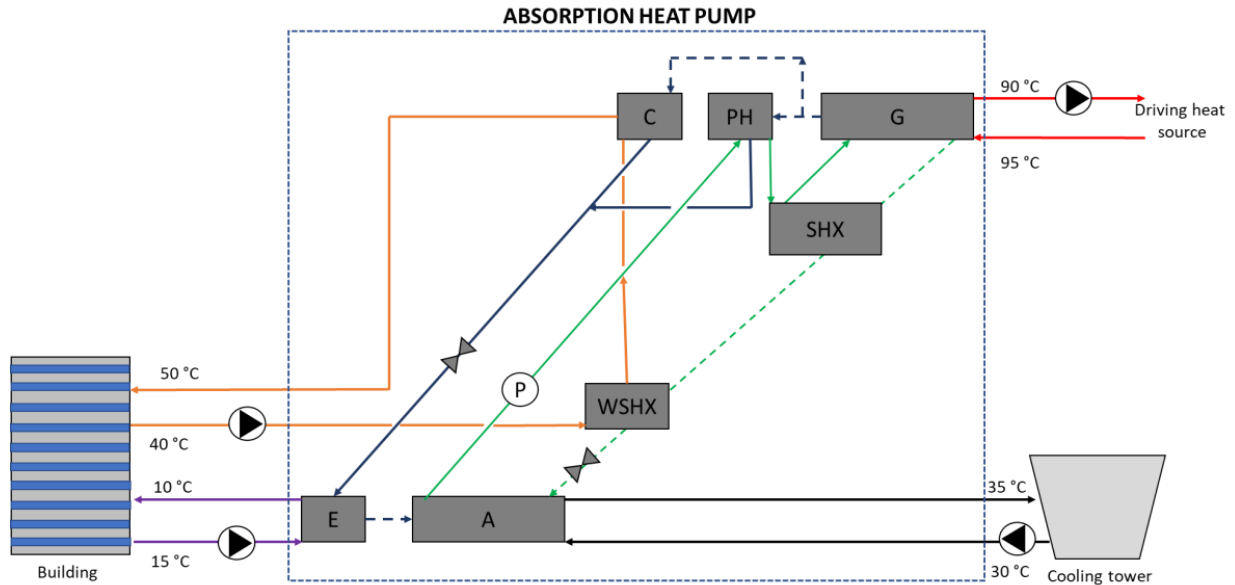


**Figure 6.** Layout for the simultaneous heating and cooling for air conditioning applications.

### 3.2. Simultaneous Heating and Cooling for 4th Generation DHC

The following application is the simultaneous heating and cooling supply for 4th Generation District Heating and Cooling networks (DHC) (Reference). Figure 7 illustrates how the proposed heat pump is integrated with this application. The proposed H<sub>2</sub>O/LiBr AHP is providing chilled water at 8 °C and hot water at 55 °C to the air conditioning system. The return temperatures are 13 °C and 30 °C for the chilled and hot water circuits, respectively.

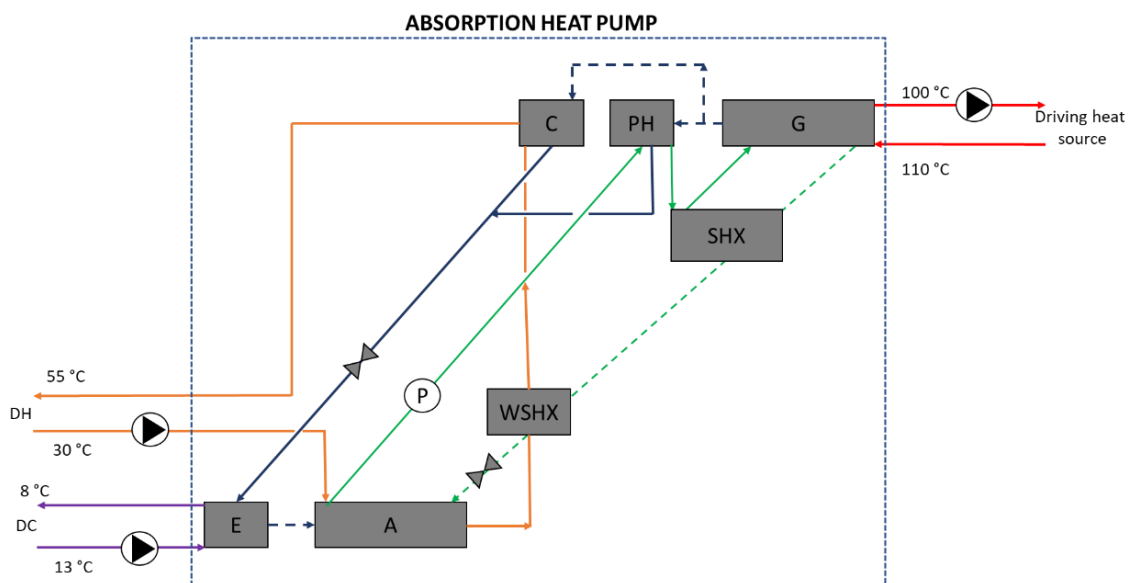


**Figure 7.** Layout for the simultaneous heating and cooling for 4th generation DHC applications.

The heat released by the absorber can be used in this application (Figure 6) since the temperature requirements of the 4th Generation DH network (i.e., inlet/outlet of 30/55 °C) are suitable for the utilization of the absorber heat along with the condenser and WSHX. Therefore, no cooling towers are required in this case. In this configuration, the hot water passes first through the absorber, then to the WSHX, and finally through the condenser. Finally, the hot water temperature required to drive the proposed H<sub>2</sub>O/LiBr AHP is 110 °C. Therefore, the driving heat source of the AHP can be provided by medium-temperature solar thermal collectors, boilers, geothermal energy, or waste heat from industries or power plants.

### 3.3. Simultaneous Heating and Cooling for a Sports Center with an Indoor Swimming Pool

The following application is the simultaneous heating and cooling for a sports center with an indoor swimming pool. Figure 8 illustrates how the proposed heat pump is integrated into this application. The H<sub>2</sub>O/LiBr AHP is providing chilled water at 10 °C, hot water at 60 °C for the DHW, and hot water to the indoor swimming pool at 32 °C. The corresponding return temperatures are 15 °C, 35 °C, and 26 °C for the chilled water circuit, the DHW circuit, and the indoor swimming pool circuit, respectively. The heat released by the absorber is used in this application since the hot water temperature requirement of the swimming pool is in the range of the absorber cooling water temperature range. Therefore, there is no need for cooling towers in this application. On the other hand, the hot water for the DHW passes first through the WSHX, and then through the condenser as depicted in Figure 7. Finally, the hot water temperature required for the driving heat is 100 °C. Therefore, the driving heat source of the proposed H<sub>2</sub>O/LiBr AHP can be provided by low /medium temperature solar thermal collectors, biomass boilers, deep geothermal resources, or waste heat from industries or CHP plants.

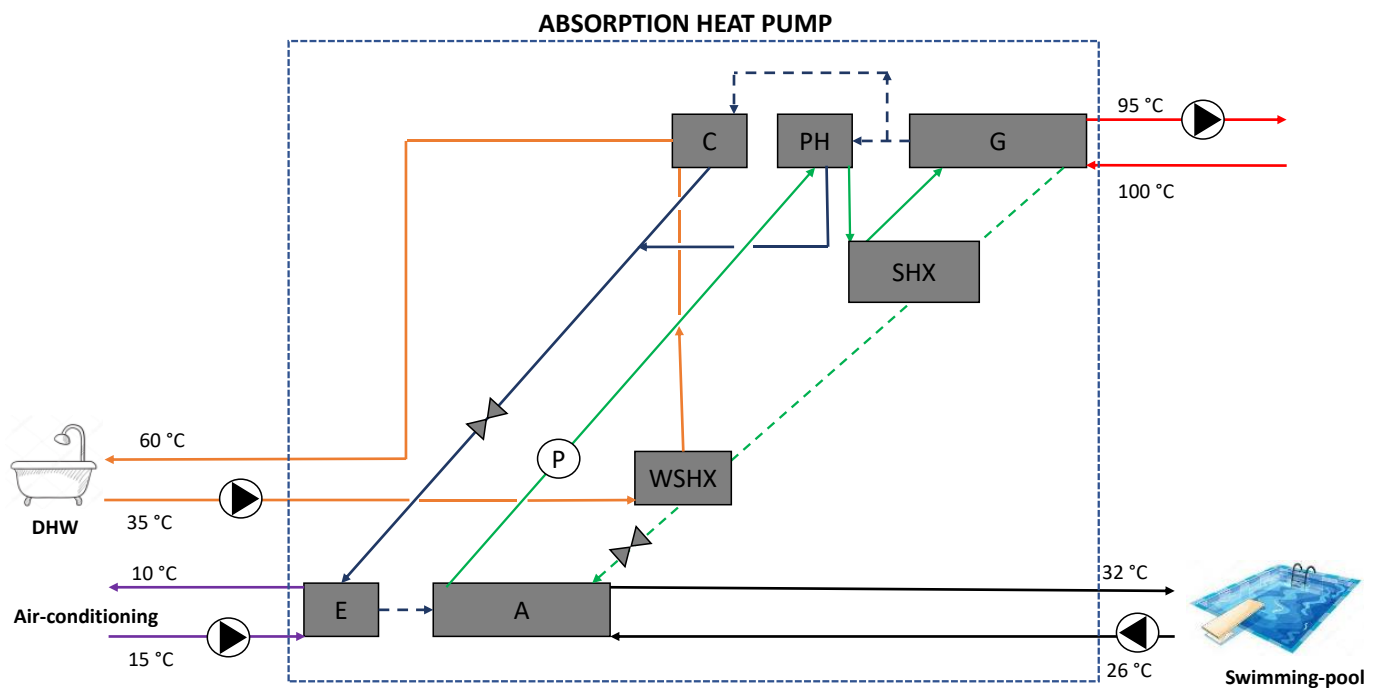


**Figure 8.** Layout for the simultaneous heating and cooling for a sports center with an indoor swimming pool application.

### 3.4. Hybrid Air Conditioning System with an Absorption Heat Pump and a Desiccant Evaporative Cooling System

The next application is a hybrid air conditioning system with an H<sub>2</sub>O/LiBr AHP and a desiccant evaporative cooling system. Figure 9 illustrates how the proposed heat pump is

integrated into this application. The  $\text{H}_2\text{O}/\text{LiBr}$  AHP is providing chilled water at  $13^\circ\text{C}$  and hot water at  $60^\circ\text{C}$  to activate the desiccant evaporative cooling system. The return temperatures are  $18^\circ\text{C}$  and  $45^\circ\text{C}$  for the chilled and hot water circuits, respectively. The chilled water supply temperature can be increased as the latent heat of the required cooling demand is handled by the desiccant system. This allows for operating the AHP at a higher evaporator temperature.

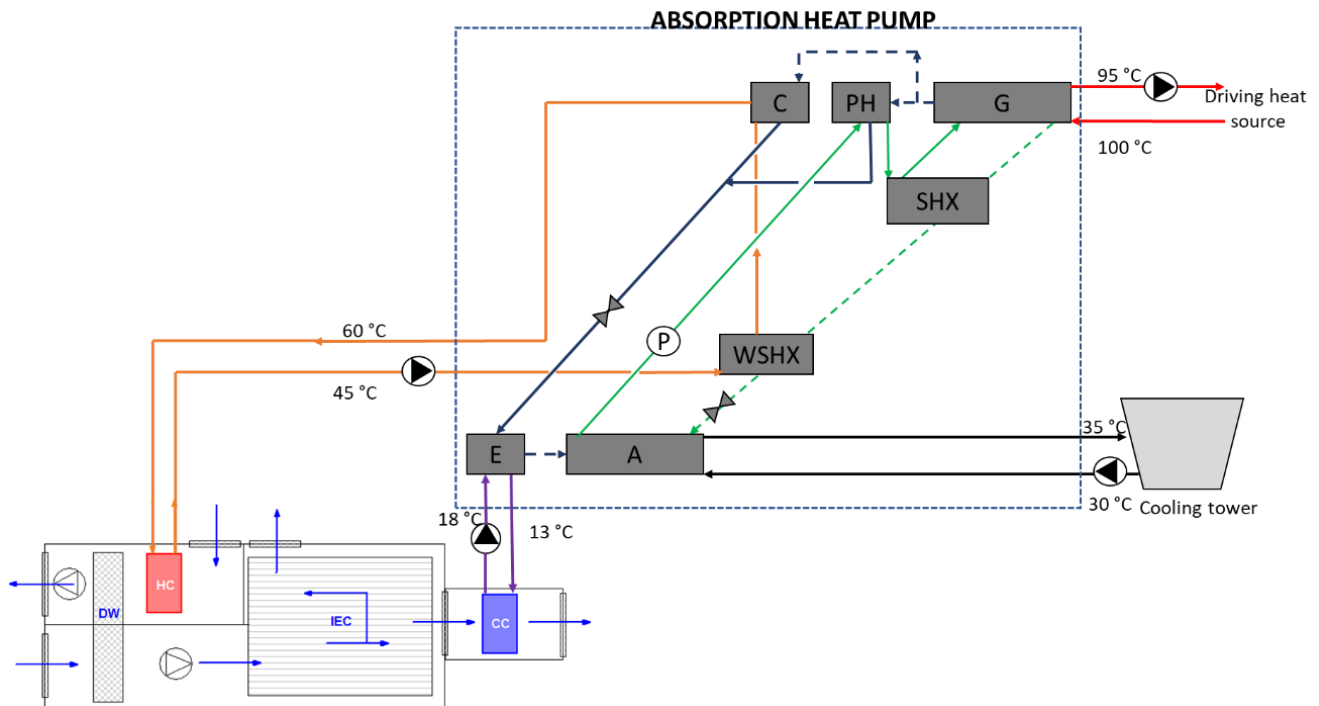


**Figure 9.** Layout for hybrid air conditioning system with an absorption heat pump and a desiccant evaporative cooling system.

The desiccant system is comprised of a desiccant wheel (DW), a heating coil (HC), and an indirect evaporative cooler (IEC), and is used to dehumidify and precool the moist air. A cooling coil (CC) cools down the air to the required supply air temperature. The cooling transferred in the CC is provided by the evaporator of the  $\text{H}_2\text{O}/\text{LiBr}$  AHP. The heat released by the absorber cannot be used in this application (Figure 8) as the temperature requirements of the desiccant system (i.e.,  $60^\circ\text{C}$ ) are higher than the heat provided by the absorber (i.e.,  $30/35^\circ\text{C}$ ). Therefore, absorber heat should be dissipated through a cooling tower. In this configuration, hot water passes first through the water–solution heat exchanger and then through the condenser. Finally, the hot water temperature required for the driving heat is  $100^\circ\text{C}$ . Therefore, the driving heat source for the AHP can be provided by low/medium temperature solar thermal collectors, biomass boilers, deep geothermal resources, or waste heat from industries or CHP plants.

### 3.5. Simultaneous Cooling and Water Purification

The last application is simultaneous cooling and water purification. Figure 10 illustrates how the proposed heat pump is integrated into this application. The  $\text{H}_2\text{O}/\text{LiBr}$  AHP is providing chilled water at  $10^\circ\text{C}$  and hot water at  $68^\circ\text{C}$  to the water purification system.

The water purification system is based on the membrane distillation (MD) process. The MD system requires a driving heat temperature in the range of  $60^\circ\text{C}$  to  $80^\circ\text{C}$  to obtain a high difference of vapor pressure across the membrane, and then high transmembrane fluxes are obtained. Therefore, the temperature of the driving heat (hot water) is set at  $70^\circ\text{C}$  for the MD water purification system. To achieve this temperature level, the feed

water is also heated by the return driving hot water of the AHP circuit as illustrated in Figure 9. An intermediate water circuit is used to transfer heat from the AHP, through the WSHX and the condenser, and the return line of the driving heat water circuit of the AHP. The heat rejected by the absorber cannot be used in this application as the temperature level required by the MD system is higher than the cooling water temperature range of the absorber. Therefore, the heat rejected by the absorber should be released to the ambient environment. In this case, seawater could be used for this purpose and, therefore, the cooling water inlet temperature in the absorber is assumed as 25 °C. Finally, the hot water temperature required for the driving heat is 110 °C. Therefore, the driving heat source for the AHP can be provided by low/medium temperature solar thermal collectors, biomass boilers, deep geothermal resources, or waste heat from industries or CHP plants.

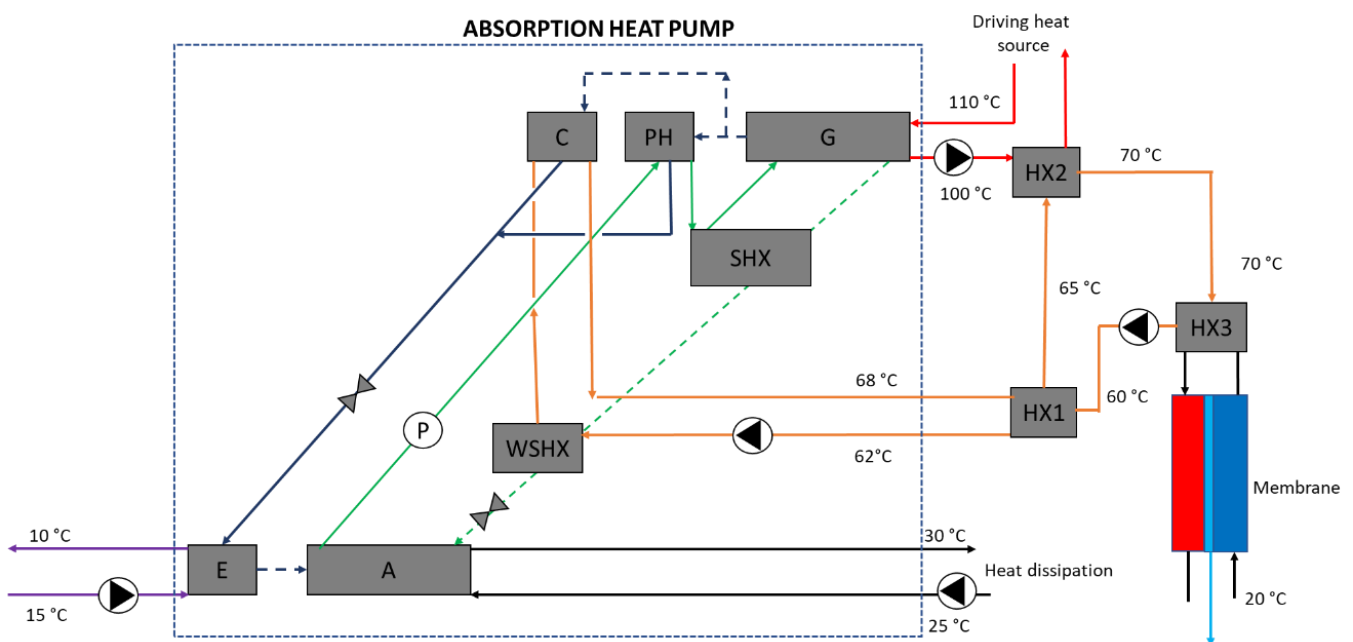


**Figure 10.** Layout for hybrid air conditioning system with an absorption heat pump and a desiccant evaporative cooling system.

### 3.6. Comparison of Applications

Figure 11 contains the required driving heat temperature for the five potential applications analyzed in this study. The applications (AC, HS, and CWP) represented with blue bars dissipate the absorber heat to the ambient environment while other applications represented with golden bars utilized the absorber heat for proposed end-use applications. Furthermore, due to the relatively higher temperatures required in the 4th Generation DHC Network (DHC) and the cooling and water purification (CWP) applications, the driving heat temperature for these two applications is 110 °C. The air conditioning application (AC) only requires 95 °C. The swimming pool (SP) and the hybrid air conditioning system (HS) need 100 °C as the driving heat temperature.

In general, these driving heat temperatures are higher than the required in the single-effect absorption chillers, which are usually lower than 95 °C to avoid the solution crystallization. If solar thermal energy is used as driving heat source, low-concentration technologies are the most suitable at these temperature levels.

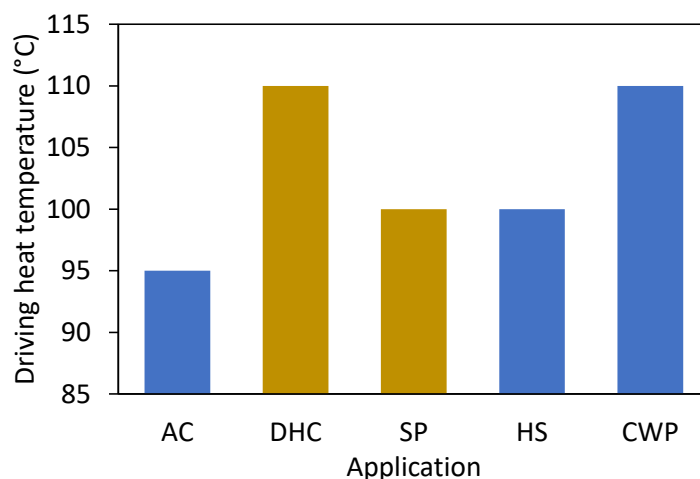


**Figure 11.** Driving heat temperature required for each application. Note: AC = air conditioning; DHC = 4th Generation District Heating and Cooling Network; SP = sports center with an indoor swimming pool; HS = hybrid air conditioning system; CWP = cooling and water purification.

#### 4. Methodology

The AHP cycle is modeled by using the Engineering Equation Solver (EES) software. The model is based on energy and mass balances on each cycle component. The thermodynamic properties of the working fluid (i.e., H<sub>2</sub>O/LiBr) are obtained using the external library “SSCLIBR.DLL” available in the EES software [23]. The temperatures of the external circuits that transfer heat to and from the cycle are related to the internal cycle temperatures by assuming a fixed typical minimum approach temperature value for each component. Moreover, the SHX and WSHX are modeled with fixed effectiveness values.

##### 4.1. Modelling Assumptions

The following modeling assumptions are made:

- The AHP cycle operates under steady-state conditions.
- Potential and kinetic energy effects are neglected.
- Pressure drops and heat losses are neglected.
- Refrigerant (water) at the exit of the condenser (stream 8) and the preheater (stream 8) is saturated conditions at the high pressure. The preheater and condenser work in a parallel flow arrangement, this means that inlet and outlet conditions are the same in both components.
- Refrigerant at the exit of the evaporator (stream 10) is saturated vapor at the low pressure.
- The H<sub>2</sub>O/LiBr solutions exiting the absorber (stream 1) and desorber (stream 4) are at saturated states at their respective temperatures and pressures.
- The refrigerant vapor leaving the desorber (stream 7) is at equilibrium with the solution coming from the absorber (stream 3).
- Counter-flow SHX and WSHX are considered.

These assumptions are very well known and are based on the assumptions taken by Herold et al. [24] for the single-effect absorption chillers.

As mentioned above, the heat exchange with the external circuit of the cycle components is modeled using typical minimum approach temperature difference values (listed in Table 2) instead of overall heat conductance (UA) values. Thereby, the corresponding UA values are obtained for sizing the components of the cycle.

**Table 2.** Minimum approach temperature difference for each cycle component.

Component	Difference of Temperatures (°C)
Evaporator	$T_{18} - T_{10} = 2.5$
Condenser	$T_8 - T_{16} = 1.0$
Absorber	$T_1 - T_{13} = 3.0$
Generator	$T_{11} - T_4 = 4.0$
Preheater	$T_8 - T_{19} = 1.0$

The SHE effectiveness value of the AHP cycle can be increased in comparison with the conventional single-effect H<sub>2</sub>O/LiBr absorption chiller since the issue of LiBr crystallization is avoided (or minimized). In this regard, the SHX effectiveness is assumed as 0.95. In addition, the WSHX effectiveness is assumed as 0.90. The weak solution flow rate is assumed as 1 kg/s.

#### 4.2. Performance Parameters

The simulated performances of the proposed H<sub>2</sub>O/LiBr AHP cycle are obtained in terms of cooling coefficient of performance ( $COP_C$ ), heating coefficient of performance ( $COP_H$ ), exergy coefficient of performance ( $ECOP$ ), and total coefficient of performance ( $COP_{tot}$ ). The  $COP_C$  is defined as the ratio of the cooling output produced by the evaporator ( $\dot{Q}_E$ ) and driving heat input in the generator ( $\dot{Q}_G$ ):

$$COP_C = \frac{\dot{Q}_E}{\dot{Q}_G} \quad (1)$$

where the cooling output produced by the evaporator ( $\dot{Q}_E$ ) and the driving heat input in the generator are calculated from their respective energy balance equations:

$$\dot{Q}_E = \dot{m}_{17} \cdot c_{p,w} \cdot (T_{17} - T_{18}) = \dot{m}_9 \cdot (h_{10} - h_9) \quad (2)$$

$$\dot{Q}_G = \dot{m}_{11} \cdot c_{p,w} \cdot (T_{11} - T_{12}) = \dot{m}_4 \cdot h_4 + \dot{m}_7 \cdot h_7 - \dot{m}_3 \cdot h_3 \quad (3)$$

The  $COP_H$  is defined as the ratio of the heating provided by the condenser ( $\dot{Q}_C$ ) and the water–solution heat exchanger ( $\dot{Q}_{WSHX}$ ) to the driving heat input in the generator ( $\dot{Q}_G$ ) for the applications where the absorber heat is dissipated to the ambient:

$$COP_H = \frac{\dot{Q}_{Co} + \dot{Q}_{WSHX}}{\dot{Q}_G} \quad (4)$$

where the heating provided by the condenser ( $\dot{Q}_C$ ) and the water–solution heat exchanger ( $\dot{Q}_{WSHX}$ ) are calculated from their respective energy balance equations:

$$\dot{Q}_{Co} = \dot{m}_{15} \cdot c_{p,w} \cdot (T_{16} - T_{15}) = \dot{m}_{8,C} \cdot (h_7 - h_8) \quad (5)$$

where  $\dot{m}_{8,C}$  is the vapor flow that is condensed in the condenser.

$$\dot{Q}_{WSHX} = \dot{m}_{21} \cdot c_{p,w} \cdot (T_{15} - T_{21}) = \dot{m}_5 \cdot (h_5 - h_{20}) \quad (6)$$

In addition, it is defined as the ratio of the heating provided by the condenser ( $\dot{Q}_C$ ), the water–solution heat exchanger ( $\dot{Q}_{WSHX}$ ), and the absorber ( $\dot{Q}_A$ ), to the driving heat

input in the generator ( $\dot{Q}_G$ ) for the applications where the absorber heat is also used for the heating applications:

$$COP_H = \frac{\dot{Q}_{Co} + \dot{Q}_{WSHX} + \dot{Q}_{abs}}{\dot{Q}_G} \quad (7)$$

where the heating provided by the absorber ( $\dot{Q}_A$ ) is calculated from the energy balance equations:

$$\dot{Q}_{abs} = \dot{m}_{13} \cdot c_{p,w} \cdot (T_{14} - T_{13}) = \dot{m}_6 \cdot h_6 + \dot{m}_{10} \cdot h_{10} - \dot{m}_1 \cdot h_1 \quad (8)$$

The  $ECOP$  of the H<sub>2</sub>O/LiBr AHP O/LiBr AHP for the applications where the absorber heat is dissipated to the ambient environment is computed as:

$$ECOP = \frac{-\dot{Q}_E \cdot \left(1 - \frac{T_0}{T_E}\right) + \dot{Q}_{Co} \cdot \left(1 - \frac{T_0}{T_{Co}}\right) + \dot{Q}_{WSHX} \cdot \left(1 - \frac{T_0}{T_{WSHX}}\right)}{\dot{Q}_G \cdot \left(1 - \frac{T_0}{T_G}\right) + W_P} \quad (9)$$

The  $ECOP$  of the H<sub>2</sub>O/LiBr AHP for the applications where the absorber heat is dissipated to the ambient environment is also used for heating applications is computed as:

$$ECOP = \frac{-\dot{Q}_E \cdot \left(1 - \frac{T_0}{T_E}\right) + \dot{Q}_{Co} \cdot \left(1 - \frac{T_0}{T_{Co}}\right) + \dot{Q}_{WSHX} \cdot \left(1 - \frac{T_0}{T_{WSHX}}\right) + \dot{Q}_{abs} \cdot \left(1 - \frac{T_0}{T_{abs}}\right)}{\dot{Q}_G \cdot \left(1 - \frac{T_0}{T_G}\right) + W_P} \quad (10)$$

where  $T_0$  is the dead state temperature (taken as 298.15 K) and the entropic average temperature of the evaporator ( $T_E$ ), condenser ( $T_C$ ), water–solution heat exchanger ( $T_{WSHX}$ ), and generator ( $T_G$ ), which are calculated using Equation (6) from the external circuits enthalpies ( $h$ ) and entropies ( $s$ ).

$$T_i = \frac{h_{i,in} - h_{i,out}}{s_{i,in} - s_{i,out}} \quad (11)$$

Finally, the combined COP ( $COP_{tot}$ ) is calculated by considering both the heating and the cooling outputs of the AHP cycle, which is defined as:

$$COP_{tot} = COP_C + COP_H \quad (12)$$

In these calculations, the pump consumption is not included due to its values being neglected in comparison with the rest of them.

## 5. Results and Discussion

The novel H<sub>2</sub>O/LiBr AHP cycle is evaluated for the five potential applications presented in Section 3. The system performance is evaluated in terms of cooling capacity, heating capacity,  $COP_C$ ,  $COP_H$ ,  $COP_{tot}$ , and  $ECOP$ . Moreover, external flow rates required for each water circuit are presented for each application.

### 5.1. Simultaneous Heating and Cooling for Air Conditioning

Figure 12 shows the working temperatures and flow rates of the simultaneous heating and cooling supplies using the novel H<sub>2</sub>O/LiBr AHP for air conditioning application.

At the same time, Table 3 contains the system performance achieved for this application. The cooling capacity and heating capacity of the AHP are 175.0 kW and 171.7 kW, respectively. These values lead to a  $COP_C$  of 0.832 and a  $COP_H$  of 0.82. Therefore, the  $COP_{tot}$  is 1.652. Finally, the  $ECOP$  achieved by the absorption heat pump is 0.475.

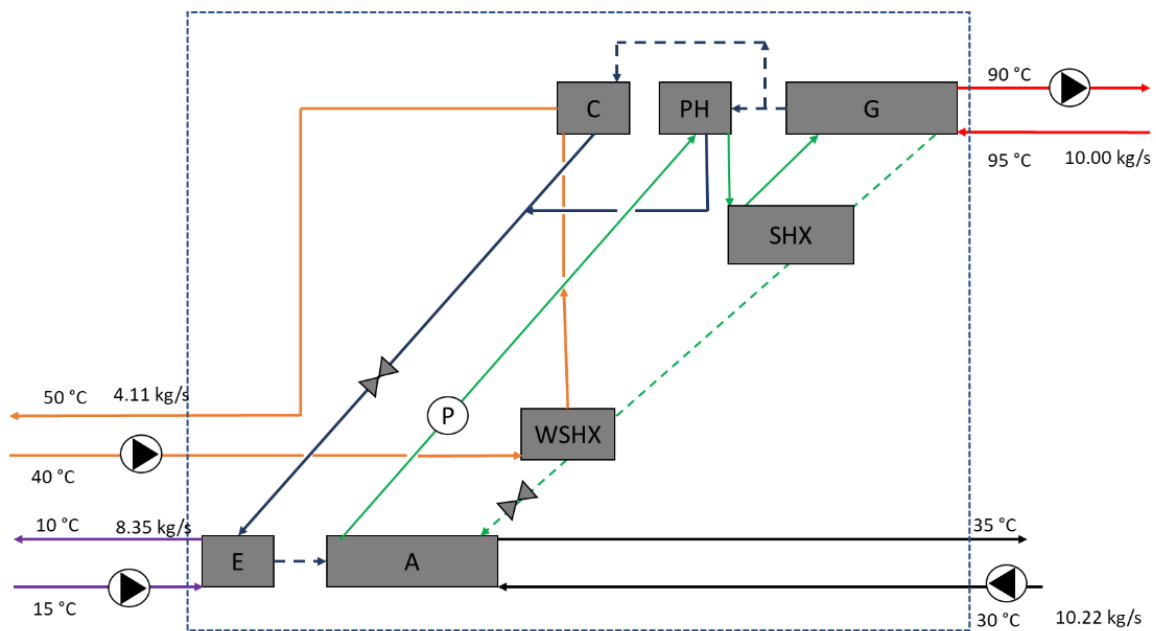


**Figure 12.** Working temperatures and flow rates for the simultaneous heating and cooling for air conditioning applications.

**Table 3.** Absorption heat pump performance for air conditioning application.

Parameter	Value
$\dot{Q}_E$ (kW)	175.0
$\dot{Q}_{Co} + \dot{Q}_{WSHX}$ (kW)	171.7
$COP_C$ (-)	0.832
$COP_H$ (-)	0.820
$COP_{tot}$ (-)	1.652
$ECOP$ (-)	0.475

### 5.2. Simultaneous Heating and Cooling for 4th Generation DHC

Figure 13 shows the working temperatures and flow rates for the simultaneous heating and cooling supplies for the 4th generation DHC application using the H<sub>2</sub>O/LiBr AHP. At the same time, Table 4 contains the system performance achieved for this application. The cooling capacity and heating capacity of the AHP are about 262.5 kW and 586 kW, respectively. In this case, the heating capacity is higher than the cooling capacity because heat released from the absorber is used for the heating applications. These values lead to a  $COP_C$  of 0.812 and a  $COP_H$  of 1.812. Therefore, the  $COP_{tot}$  is 2.624. Finally, the  $ECOP$  achieved by the AHP is 0.667.

**Table 4.** Absorption heat pump performance for 4th Generation DHC.

Parameter	Value
$\dot{Q}_E$ (kW)	262.5
$\dot{Q}_{Co} + \dot{Q}_{abs} + \dot{Q}_{WSHX}$ (kW)	586.0
$COP_C$ (-)	0.812
$COP_H$ (-)	1.812
$COP_{tot}$ (-)	2.624
$ECOP$ (-)	0.667

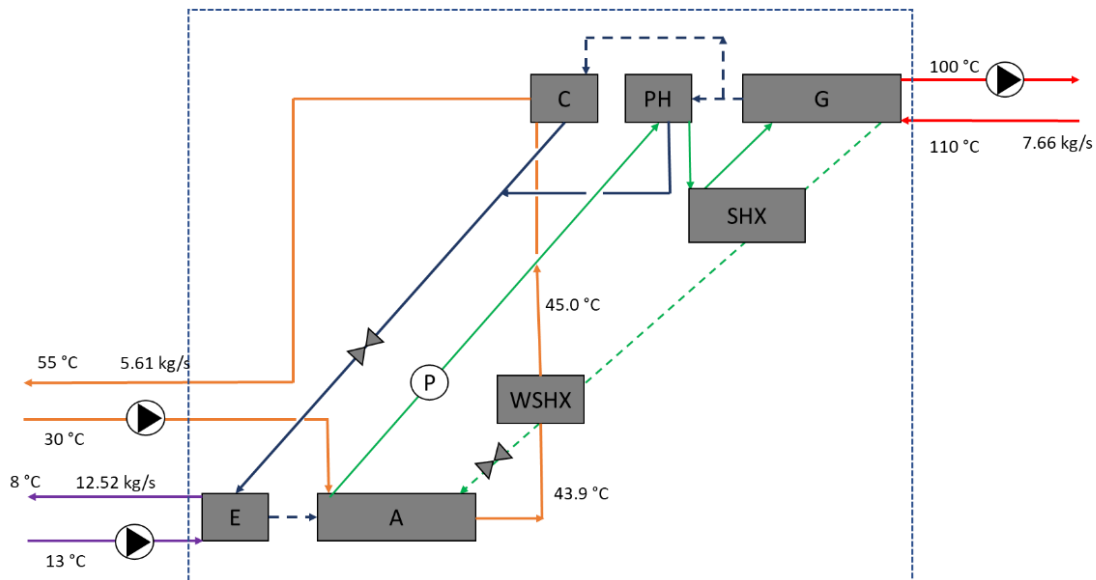


**Figure 13.** Working temperatures and flow rates for the simultaneous heating and cooling for 4th generation DHC application.

5.3. Simultaneous Heating and Cooling for a Sports Center with an Indoor Swimming Pool

Figure 14 shows the working temperatures and flow rates for the simultaneous heating and cooling supplies using the H<sub>2</sub>O/LiBr AHP for a sports center with an indoor swimming pool. At the same time, Table 5 contains the system performance achieved for this application. The cooling capacity and heating capacity of the AHP are 154.0 kW and 336.9 kW, respectively. In this case, the heating capacity is higher than the cooling capacity because heating from the absorber can be used to heat the swimming pool. These values lead to a  $COP_{Co}$  of 0.842 and a  $COP_H$  of 1.842. Therefore, the  $COP_{tot}$  is 2.684. Finally, the  $ECOP$  achieved by the absorption heat pump is 0.54.

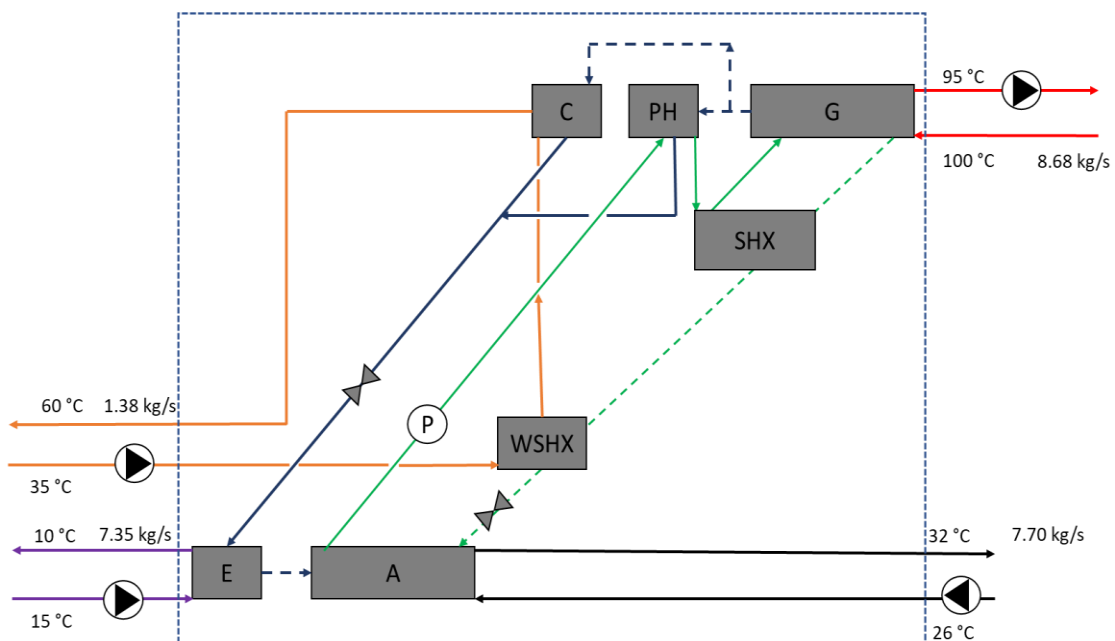


**Figure 14.** Working temperatures and flow rates for the simultaneous heating and cooling for a sports center with an indoor swimming pool.

**Table 5.** Absorption heat pump performance for an indoor swimming pool.

Parameter	Value
$\dot{Q}_E$ (kW)	154.0
$\dot{Q}_{Co} + \dot{Q}_{abs} + \dot{Q}_{WSHX}$ (kW)	336.9
$COP_C$ (-)	0.842
$COP_H$ (-)	1.842
$COP_{tot}$ (-)	2.684
$ECOP$ (-)	0.540

**5.4. Hybrid Air Conditioning System with an Absorption Heat Pump and a Desiccant Evaporative Cooling System**

Figure 15 shows the working temperatures and flow rates for the hybrid air conditioning system with an AHP and a desiccant evaporative cooling system application. At the same time, Table 6 contains the system performance achieved for this application. The cooling capacity and heating capacity of the AHP are about 137.8 kW and 117.9 kW, respectively. These values lead to a  $COP_C$  of around 0.840 and a  $COP_H$  of 0.720. Therefore, the  $COP_{tot}$  is 1.560. Finally, the  $ECOP$  achieved by the AHP is about 0.451.

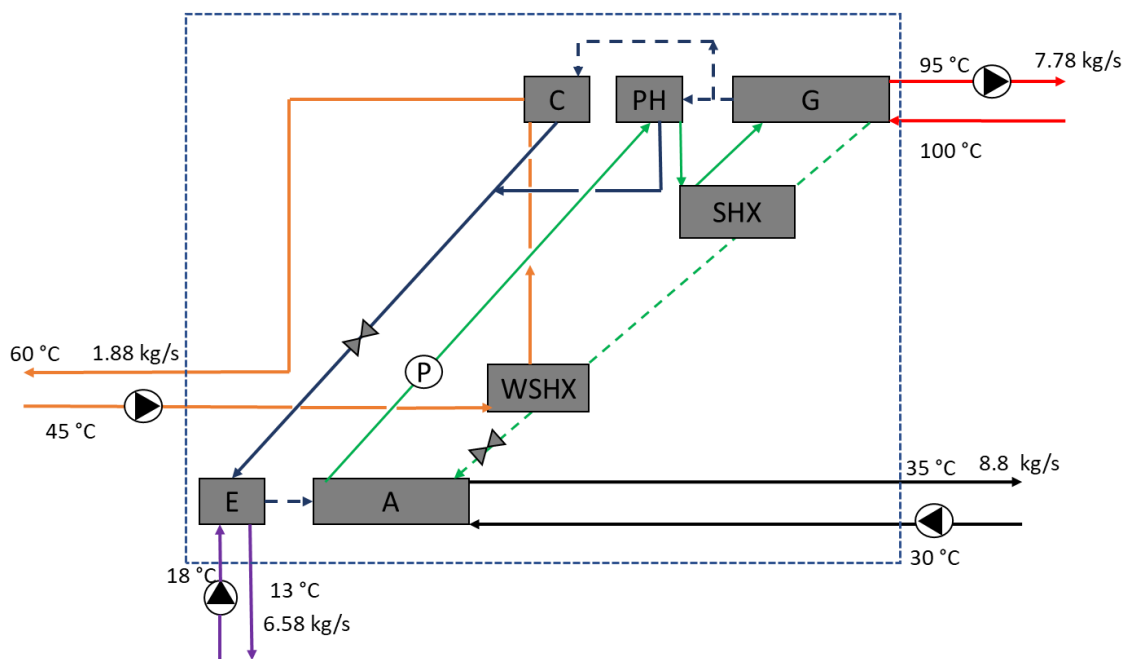


**Figure 15.** Working temperatures and flow rates for the hybrid air conditioning system.

**Table 6.** Absorption heat pump performance for the hybrid air conditioning system.

Parameter	Value
$\dot{Q}_E$ (kW)	137.8
$\dot{Q}_{Co} + \dot{Q}_{WSHX}$ (kW)	117.9
$COP_C$ (-)	0.840
$COP_H$ (-)	0.720
$COP_{tot}$ (-)	1.560
$ECOP$ (-)	0.451

**5.5. Simultaneous Cooling and Water Purification**

Figure 16 shows the working temperatures and flow rates for the simultaneous cooling and water purification application. At the same time, Table 7 contains the system perfor-

mance achieved for this application. The cooling capacity and heating output obtained for water purification using the H<sub>2</sub>O/LiBr AHP are about 193.8 kW and 134.1 kW, respectively. These values lead to a  $COP_C$  of 0.838 and a  $COP_H$  of 0.58 obtained for the AHP. Therefore, the  $COP_{tot}$  is about 1.418. Finally, the  $ECOP$  achieved by the AHP is 0.485.

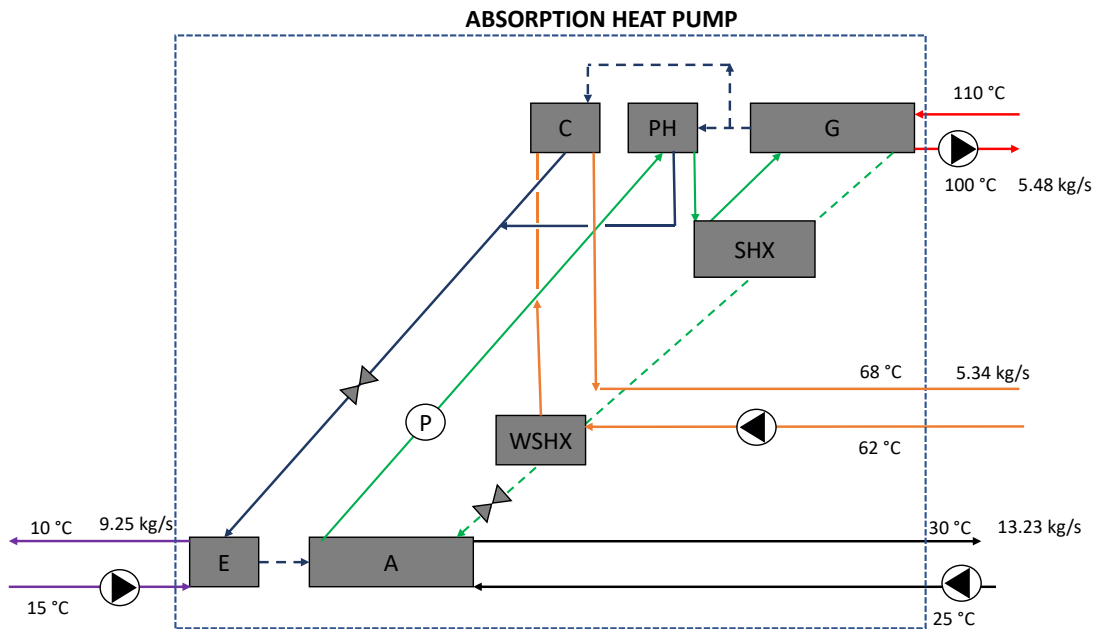


**Figure 16.** Working temperatures and flow rates for the simultaneous heating and cooling for air conditioning applications.

**Table 7.** Absorption heat pump performance for cooling and water purification.

Parameter	Value
$\dot{Q}_E$ (kW)	193.8
$\dot{Q}_{Co} + \dot{Q}_{WSHX}$ (kW)	134.1
$COP_C$ (-)	0.838
$COP_H$ (-)	0.580
$COP_{tot}$ (-)	1.418
$ECOP$ (-)	0.485

### 5.6. Comparison of Applications

In order to evaluate the application where the proposed H<sub>2</sub>O/LiBr AHP performs in a better way, the  $ECOP$  is used as it considers not only the useful energy outputs achieved by the system but also the quality of both the energy required and the energy provided by the AHP. Therefore, Figure 17 summarizes the  $ECOP$  of the AHP for the five potential applications evaluated. In Figure 16, the applications represented with blue bars dissipate the absorber heat to the ambient environment, while applications represented with golden bars use the heat released by the absorber for the heating applications.

The two applications with the highest  $ECOP$  are the DHC and the SP, as these applications can use the heat released by the absorber for the heating application. Despite the  $COP_{tot}$  being lower in the DHC application than in the SP application, the  $ECOP$  achieved by the DHC application is significantly higher due to the higher heating temperature in the absorber. The three applications with the lowest  $ECOP$  are the AC, the HS, and the CWP, as these applications cannot use the heat rejected by the absorber for heating applications. In these applications, the  $ECOP$  of the AHP is similar, despite the working temperatures being different among them.

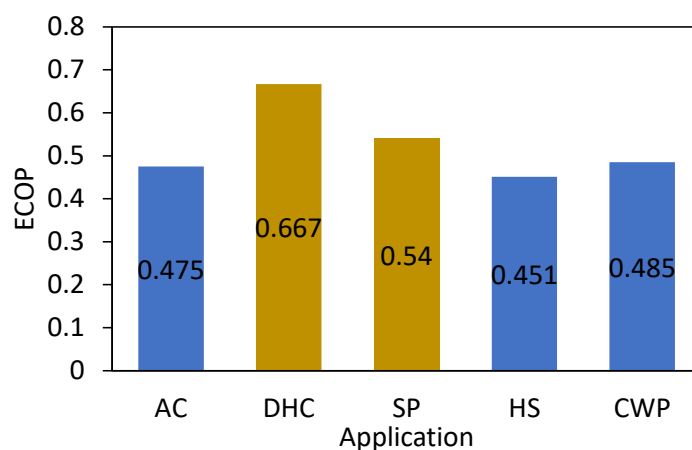


**Figure 17.** *ECOP* achieved for each application.

Therefore, the *ECOP* ranges from 0.451 in the HS to 0.667 in the DHC; this corresponds to an *ECOP* increase of 48% for the latest.

## 6. Conclusions and Future Works

A novel AHP was proposed in this paper. This heat pump was based on a single-effect H<sub>2</sub>O/LiBr absorption chiller and was modified for the combined production of cooling and heating by recovering the condensation heat at a useful temperature level instead of rejecting it to ambient air, as in the case of a conventional single-effect absorption chiller. Furthermore, part of the heat of condensation was recovered internally to preheat the weak H<sub>2</sub>O/LiBr solution. The main changes that the AHP cycle requires in comparison with the conventional single-effect absorption chiller were described. Operational limitations of the cycle were set in terms of maximum and minimum driving heat temperatures for different set chilled and hot water supply temperatures. The minimum and maximum driving heat temperatures required by this AHP are from 85 °C to 120 °C, which are, in general, higher than those required by the conventional single-effect H<sub>2</sub>O/LiBr absorption chiller.

Increasing the solution heat exchanger effectiveness allows for an increase of the AHP performance, especially the  $COP_C$ , which increases from 0.7 to 0.83. The novel H<sub>2</sub>O/LiBr AHP was evaluated under five potential applications that require simultaneous heating and cooling: an air conditioning application, a 4th generation DHC network, a sports center with an indoor swimming pool, a hybrid air conditioning system with an AHP and a desiccant evaporative cooling system, and a simultaneous cooling and water purification application. For these five applications, the novel AHP showed promising results, especially for the 4th generation DHC, and the sports center with an indoor swimming pool, where heat rejected from the absorber can also be used for the heating application. In these two applications the  $COP_C$  is 0.812 and 0.842, the  $COP_H$  is 1.812 and 1.842, and the *ECOP* is 0.667 and 0.54, respectively. In the other three applications, where the heat rejected from the absorber cannot be used, the  $COP_C$  ranges between 0.832 and 0.840. The  $COP_H$  is smaller in these cases: 0.58 in the CWP, 0.72 in the HS, and 0.82 in the AC. The *ECOP* ranges between 0.451 and 0.485.

Future work will be an experimental evaluation at the laboratory level of a complete AHP. This evaluation will be helpful to validate the novel AHP and identify possible issues to be solved before its integration in a demonstration site.

## 7. Patents

- Patent application (Spanish patent): 202230332
- Title: “Bomba de calor de absorción de agua-bromuro de litio para producción simultánea de frío y calor”

- Patent inventors: Alberto Coronas Salcedo, Juan Prieto González, and José Ignacio Ajona Maeztu
- Patent beneficiaries: Universitat Rovira i Virgili, José Ignacio Ajona Maeztu
- S/Ref.: N/Ref.: 2022/6714

**Author Contributions:** Conceptualization, J.P. and A.C.; methodology, J.P. and D.S.A.; formal analysis, J.P.; investigation, J.P.; writing—original draft preparation, J.P. and D.S.A.; writing—review and editing, D.S.A. and A.C.; supervision, A.C.; project administration, A.C.; funding acquisition, A.C. All authors have read and agreed to the published version of the manuscript.

**Funding:** This work has been supported by the European WEDISTRICT project (grant agreement No. 857801) co-founded by the EC under the call H2020-LC-SC3-2018-2019-2020 and by the Tarragona Provincial Council under the collaboration framework agreement between the Tarragona Provincial Council and the Rovira i Virgili University for the period 2020–2023 with the reference number 2022/#.

**Institutional Review Board Statement:** Not applicable.

**Informed Consent Statement:** Not applicable.

**Data Availability Statement:** Not applicable.

**Conflicts of Interest:** The authors declare no conflict of interest.

## Nomenclature

$COP$	Coefficient of performance (-)
$ECOP$	Exergy coefficient of performance (-)
$h$	Specific enthalpy ( $\text{kJ}\cdot\text{kg}^{-1}$ )
$\dot{m}$	Mass flow rate ( $\text{kg}\cdot\text{s}^{-1}$ )
$q$	Vapor quality (-)
$Q$	Heating or cooling rate (kW)
$s$	Specific entropy ( $\text{kJ}\cdot\text{kg}^{-1}\cdot\text{K}^{-1}$ )
$T$	Temperature ( $^{\circ}\text{C}$ )
$p$	Pressure (kPa)
$x$	LiBr mass fraction (-)
Greeks	
$\eta$	Effectiveness (-)
Subscripts	
$abs$	Absorber
$C$	Cooling
$chi$	Chilled water
$Co$	Condenser
$E$	Evaporator
$G$	Generator
$H$	Heating
$HX$	Solution heat exchanger
$in$	Inlet
$max$	Maximum
$min$	Minimum
$WSHX$	Water-solution heat exchanger

## References

1. Gerard, F.; Guevara Opinska, L.; Smit, T.; Rademaekers, K.; Braungardt, S.; Montagud, M.E.M. *Policy Support for Heating and Cooling Decarbonisation-Roadmap*; European Commission: Brussels, Belgium, 2022. [[CrossRef](#)]
2. Bienvenido-Huertas, D.; Pulido-Arcas, J.A.; Rubio-Bellido, C.; Pérez-Fargallo, A. Feasibility of adaptive thermal comfort for energy savings in cooling and heating: A study on Europe and the Mediterranean basin. *Urban Clim.* **2021**, *36*. [[CrossRef](#)]
3. Ghoubali, R.; Byrne, P.; Miriel, J.; Bazantay, F. Simulation study of a heat pump for simultaneous heating and cooling coupled to buildings. *Energy Build* **2014**, *72*, 141–149. [[CrossRef](#)]

4. Byrne, P.; Ghoubali, R. Exergy analysis of heat pumps for simultaneous heating and cooling. *Appl. Therm. Eng.* **2019**, *149*, 414–424. [[CrossRef](#)]
5. Kuyumcu, M.E.; Tutumlu, H.; Yumrutaş, R. Performance of a swimming pool heating system by utilizing waste energy rejected from an ice rink with an energy storage tank. *Energy Convers. Manag.* **2016**, *121*, 349–357. [[CrossRef](#)]
6. Ramírez, C.A.; Patel, M.; Blok, K. From fluid milk to milk powder: Energy use and energy efficiency in the European dairy industry. *Energy* **2006**, *31*, 1984–2004. [[CrossRef](#)]
7. Liu, Y.; Groll, E.A.; Yazawa, K.; Kurtulus, O. Theoretical analysis of energy-saving performance and economics of CO<sub>2</sub> and NH<sub>3</sub> heat pumps with simultaneous cooling and heating applications in food processing. *Int. J. Refrig.* **2016**, *65*, 129–141. [[CrossRef](#)]
8. Liu, Y.; Groll, E.A.; Yazawa, K.; Kurtulus, O. Energy-saving performance and economics of CO<sub>2</sub> and NH<sub>3</sub> heat pumps with simultaneous cooling and heating applications in food processing: Case studies. *Int. J. Refrig.* **2017**, *73*, 111–124. [[CrossRef](#)]
9. Byrne, P.; Fournaison, L.; Delahaye, A.; Oumeziane, Y.A.; Serres, L.; Loulergue, P.; Szymczyk, A.; Mugnier, D.; Malaval, J.L.; Bourdais, R.; et al. A review on the coupling of cooling, desalination and solar photovoltaic systems. *Renew. Sustain. Energy Rev.* **2015**, *47*, 703–717. [[CrossRef](#)]
10. Eisa, M.A.R.; Devotta, S.; Holland, F.A. Thermodynamic design data for absorption heat pump systems operating on water-lithium bromide: Part III-Simultaneous cooling and heating. *Appl. Energy* **1986**, *25*, 83–96. [[CrossRef](#)]
11. Kumar, P.; Sane, M.G.; Devotta, S.; Holland, F.A. Experimental studies with an absorption system for simultaneous cooling and heating. *Chem. Eng. Res. Des.* **1985**, *63*, 133–136.
12. Best, R.; Riviera, W.; Pilatowsky, I.; Holland, F.A.; Engineering, G. Thermodynamic design data for absorption heat pump systems operating on Ammonia-Lithium Nitrate-Part Three. Simultaneous cooling and heating. *Heat Recover. Syst. CHP* **1991**, *11*, 199–212. [[CrossRef](#)]
13. Best, R.; Rvera, W.; Oskam, A. Thermodynamic design data for absorption heat pump systems operating on water-carrol. Part III: Simultaneous cooling and heating. *Heat Recover. Syst. CHP* **1995**, *15*, 445–456. [[CrossRef](#)]
14. Fathalah, K.; Aly, S.E. Theoretical study of a solar powered absorption/MED combined system. *Energy Convers. Manag.* **1991**, *31*, 529–544. [[CrossRef](#)]
15. Elshamarka, S. Absorption Heat Pump for a Potable Water Supply in a Solar House. *Appl. Energy* **1991**, *40*, 31–40. [[CrossRef](#)]
16. Gude, V.G.; Nirmalakhandan, N. Combined desalination and solar-assisted air-conditioning system. *Energy Convers. Manag.* **2008**, *49*, 3326–3330. [[CrossRef](#)]
17. Wang, Y.; Lior, N. Combined desalination and refrigeration systems driven by low-grade heat. In Proceedings of the ASME International Mechanical Engineering Congress and Exposition, Boston, MA, USA, 31 October–6 November 2008.
18. Wang, Y.; Lior, N. Proposal and analysis of a high-efficiency combined desalination and refrigeration system based on the LiBr-H<sub>2</sub>O absorption cycle—Part 1: System configuration and mathematical model. *Energy Convers. Manag.* **2011**, *52*, 220–227. [[CrossRef](#)]
19. Wang, Y.; Lior, N. Proposal and analysis of a high-efficiency combined desalination and refrigeration system based on the LiBr-H<sub>2</sub>O absorption cycle—Part 2: Thermal performance analysis and discussions. *Energy Convers. Manag.* **2011**, *52*, 228–235. [[CrossRef](#)]
20. Ibrahim, A.G.M.; Dincer, I. Experimental performance evaluation of a combined solar system to produce cooling and potable water. *Sol. Energy* **2015**, *122*, 1066–1079. [[CrossRef](#)]
21. Boman, D.B.; Garimella, S. Absorption heat pump cycles for simultaneous space conditioning and graywater purification. *Appl. Therm. Eng.* **2020**, *167*, 114587. [[CrossRef](#)]
22. Boman, D.B.; Garimella, S. Design and experimental demonstration of enabling components for simultaneous water purification and space conditioning using thermally driven absorption heat pumps. *Appl. Therm. Eng.* **2022**, *201*, 117752. [[CrossRef](#)]
23. LiBr-Water Library. Sorption Systems Consortium at the University of Maryland. Available online: <https://fchartsoft-ware.com/ees/eeshelp/hs730.htm> (accessed on 14 October 2022).
24. Herold, K.E.; Radermacher, R.; Klein, S.A. *Absorption Chillers and Heat Pumps*, 2nd ed.; Taylor & Francis Group: New York, NY, USA, 2016; ISBN 13: 978-1-4987-1435-8.

**Disclaimer/Publisher's Note:** The statements, opinions and data contained in all publications are solely those of the individual author(s) and contributor(s) and not of MDPI and/or the editor(s). MDPI and/or the editor(s) disclaim responsibility for any injury to people or property resulting from any ideas, methods, instructions or products referred to in the content.